Evaluation of the Effect of Natural Stone Processing Waste Incorporation on Red Ceramics Physical Properties

Maria Catarina Menegucci Lougon, Carla Therezinha Dalvi Borjaille Alledi & André Gustavo de Sousa Galdino

Instituto Federal do Espírito Santo

ABSTRACT

Industrial growth and the development of societies have led to increased waste generation and environmental degradation. Consequently, there have been attempts to search for alternative ways of reusing waste materials. Studies aimed at the insertion of these residues into ceramic materials are currently ongoing, partially because of the perceived potential for their suitability in this industrial branch. In this context, the present work aims to verify the potential use of the residue generated from a sludge that is an abundant byproduct of the processing of natural stone and that is difficult to discard. The study considers the use of this sludge as raw material in the development of a ceramic mass that is used in the manufacture of coatings, blocks, tiles, and bricks, among other applications. The residue from natural stone processing is then incorporated into the ceramic mass as a partial substitute for the less plastic clay of a standard mixture used in the ceramic industry located in the northwestern state of Espírito Santo (ES), Brazil. The characterization of the raw materials, clays, and residue was performed by X-ray diffraction, X-ray fluorescence, scanning electron microscopy, thermogravimetric analysis, differential scanning calorimetry, granulometric analysis, and plasticity index. Mixtures containing clays and residue were prepared, and from them cylindrical specimens were molded by the application of uniaxial pressure. Sintering of the specimens was conducted at temperatures similar to those used in the red ceramics industries, i.e., at 850°C, 900°C, and 950°C.

Keywords: clay; red ceramic; natural stone waste.

Classification: FOR Code: 091399

Language: English

London Journals Press

LJP Copyright ID: 392831
Print ISSN: 2631-8474
Online ISSN: 2631-8482

London Journal of Engineering Research

Volume 19 | Issue 1 | Compilation 1.0

Evaluation of the Effect of Natural Stone Processing Waste Incorporation on Red Ceramics Physical Properties

Maria Catarina Menegucci Lougon[α], Carla Therezinha Dalvi Borjaille Alledi[σ] & André Gustavo de Sousa Galdino[ρ]

ABSTRACT

Industrial growth and the development of societies have led to increased waste generation and environmental degradation. Consequently, there have been attempts to search for alternative ways of reusing waste materials. Studies aimed at the insertion of these residues into ceramic materials are currently ongoing, partially because of the perceived potential for their suitability in this industrial branch. In this context, the present work aims to verify the potential use of the residue generated from a sludge that is an abundant byproduct of the processing of natural stone and that is difficult to discard. The study considers the use of this sludge as raw material in the development of a ceramic mass that is used in the manufacture of coatings, blocks, tiles, and bricks, among other applications. The residue from natural stone processing is then incorporated into the ceramic mass as a partial substitute for the less plastic clay of a standard mixture used in the ceramic industry located in the northwestern state of Espírito Santo (ES), Brazil. The characterization of the raw materials, clays, and residue was performed by X-ray diffraction, X-ray fluorescence, scanning electron microscopy, thermogravimetric analysis, differential scanning calorimetry, granulometric analysis, and plasticity index. Mixtures containing clays and residue were prepared, and from them cylindrical specimens were molded by the application of uniaxial pressure. Sintering of the specimens was conducted at temperatures similar to those used in the red ceramics industries, i.e., at 850°C, 900°C, and 950°C. Physical tests were performed to determine the indices of water absorption, apparent porosity, apparent density, linear firing shrinkage, and compressive strength. The results obtained were analyzed to identify possible outliers, and the five most scattered results were eliminated. The experimental results indicate a potential for obtaining ceramic masses with technological properties that are comparable with those of masses employed for the production of the reference red ceramics.

Keywords: clay; red ceramic; natural stone waste.

*Author*α σ ρ: Instituto Federal de Pesquisa, Ciência e Tecnologia do Espírito Santo, Av. Vitória, 1729, Jucutuquara, Vitória, ES, 29040-780.

I. INTRODUCTION

Brazil is one of the main producers of natural stone and the sixth largest exporter after Italy, China, India, Spain, and Portugal (Sardou Filho et al., 2015). During the processing, natural stone is cut by steel grits or by diamond wire. The cutting of natural rock generates a residue that can have 50% of the mass of the volume of pieces produced. This residue is rich in constituents such as SiO_2, Al_2O_3, Fe_2O_3, CaO, K_2O, and Na_2O, which are also present in various raw materials used for the manufacture of construction products such as clays. The residue therefore has a potential for use as an additive in the manufacture of products such as bricks, ceramic blocks, and tiles. The incorporation of this residue has been the subject of several studies, both for red ceramic products

London Journal of Engineering Research

(Menezes et al., 2008; Boltakova et al., 2017; Zhang, 2013; Hossiney et al., 2018; Menezes et al., 2005; Segadães et al., 2005; Torres et al., 2009; Vieira et al., 2004; Coletti et al., 2018; Acchar et al., 2006) and for other products (Yeşilaya et al., 2017; Nunes et al., 2014; Marras et al., 2017; Aydin et al., 2017; Ribeiro et al., 2017; Alyamac et al., 2017; Dondi et al., 2016; Medina et al., 2017; André et al., 2014; Sardinha et al., 2016; Soltan et al., 2016; Lu et al., 2018).

The use of such waste as a raw material or as a total or partial replacement of the raw material is important because this approach would reduce the environmental impact associated with the use of deposits or with the extraction of clay from the environment. However, few studies report on the use of the cutting residue of natural rock in the presence of sawdust, and show how such a residue interferes with the physical and chemical properties of red ceramic products.

This work aims to evaluate the influence of the residue from the cutting of natural rock on the physical properties of ceramic masses composed of clay.

II. MATERIALS AND METHODS

2.1 Materials

The raw materials used to make test specimens were clays, which were kindly provided by the company Cerâmica Adélio Lubiana Ltd. (in Nova Venécia, ES, Brazil), and residues from the sludge from granite processing, which were provided by the Waste Treatment Center (CTR) (also located in Nova Venécia, ES, Brazil).

Two different clays were collected for the experiment, one that has more plasticity and one with a lower plasticity index (PI) according to the production process of the ceramic industry supplying the material. The more plastic clay was given the nomenclature sample A, while the clay with a lower plasticity was denoted sample B. The residue (R) in powder form was collected at the CTR from an area where materials are destined for the landfill after having been passed through a filter press. The residue was not subjected to any process for the removal of metallic iron, thereby maintaining the entire metallic fraction.

2.2 Methods

2.2.1 Characterization and processing of raw materials

The clays and the residue were characterized by Atterberg indices, granulometry, X-ray fluorescence (XRF) limits, and thermal analysis. To prepare for this, the samples were dried under mild conditions (at 25°C) to preserve any organic matter that may have been present in the material. After the natural drying, each material was discharged into a mortar and passed through an ABNT No. 80 sieve (0.177 mm). Samples A, B, and R were then placed in an oven at 110°C for 24 h for the removal of free and adsorbed water, and they were then discharged into a mortar and passed through an ABNT No. 80 (0.177 mm) sieve.

2.2.2 Determination of samples

In this study, three samples were adopted for the analysis, namely the reference sample (TR) (3A-4B), the T1 sample (3A-3B-1R), and the T2 sample (3A-2B-2R). Table 1 shows the composition of the samples with the corresponding percentages by volume.

Table 1: Composition of TR, T1, and T2 samples

Raw materials	TR (%)	T1 (%)	T2 (%)
Clay A	43	43	43
Clay B	57	43	28.5
Natural stone residue (R)	-	14	28.5
Composition	3A-4B	3A-3B-1	3A-2B-2

The TR sample was used as a reference because this is one of the compositions adopted by the supplier of the ceramic material. Samples TR, T1, and T2 were each mixed and homogenized manually.

2.2.3 Granulometric analysis

The granulometric distributions of samples A, B, and R and samples TR, T1, and T2 were performed in the Malvern Mastersizer Hydro 2000 MU apparatus of the Laboratory of Ceramic Materials of the Federal Institute of Espírito Santo (IFES) Vitória campus.

2.2.4 Plasticity analysis

The plastic properties of samples A and B and samples TR, T1, and T2 were determined by analyzing the liquidity limit (LL), plasticity limit (PL), and plasticity index (PI) according to technical standards NBR 6459 (ABNT, 2017) and NBR 7180 (ABNT, 2016).

The PI is given by Equation (1).

$$PI = LL - PL \quad (1)$$

2.2.5 X ray–diffraction analysis

The qualitative mineralogical analysis of the minerals present in samples A, B, and R was performed by X-ray diffraction (XRD). The analyses were conducted in a Bruker D8 Advance diffractometer operated at a power of 40 kV / 20 A with an incident radiation of Cu (λkα) and with the diffracted beam monochromatized by a curved graphite monochromator. Samples were measured in the range of 2θ: 10–100° in continuous scan mode at a rate of 1.5°/min in increments of 0.02° at ambient temperature (23°C).

2.2.6 Thermal analysis

Samples A, B, and R were submitted to thermogravimetric analysis (TG) and differential scanning calorimetry (DSC) tests. The assay was conducted in a nitrogen atmosphere from ambient temperature up to 1050°C with a heating rate of 10 K/min.

2.2.7 Chemical composition analysis

The chemical analyses of samples A, B, and R were performed using X-ray fluorescence (XRF) spectrometer coupled to a computer for data processing. This study was conducted at the Federal University of Campina Grande.

2.2.8 Morphological characterization

The morphologies of samples A, B, and R and samples TR, T1, and T2 were observed by scanning electron microscopy (SEM). Samples and powder samples were oven-dried at 110°C for 24 h and submitted for analysis. The SEM analyses were performed at the IFES Vitória campus using a Zeiss EVO MA 10 device.

2.2.9 Preparation and sintering of specimens

Cylindrical specimens of samples TR, T1, and T2 (12 mm in diameter and 24 mm in height) were made by uniaxial pressing with a single-piston action of 20 kN. Sintering of the specimens was conducted in a muffle furnace with a heating rate of 5°C/min, with sintering temperatures of 850°C, 900°C, and 950°C maintained for 2 h, and with natural cooling by turning off the oven. These temperatures were chosen because they represent the range of firing temperatures used by the red ceramic industries.

2.2.10 Physical and mechanical characterization of specimens

The test specimens were submitted to physical tests of moisture content (MC) and linear drying shrinkage (LDS) after pressing and tests of water absorption (WA), apparent porosity (AP), apparent density (AD), linear firing shrinkage (LFS), and compressive strength (CS) after firing. The results of the physical tests were obtained through the arithmetic average of 20 test specimens, and were calculated using Equations (2) to (8) as follows.

$$MC\ (\%) = \left(\frac{W_w - W_d}{W_d}\right).100 \quad (2)$$

$$LDS\ (\%) = \left(\frac{L_0 - L_d}{L_0}\right).100 \quad (3)$$

$$WA\ (\%) = \left(\frac{W_2 - W_1}{W_1}\right).100 \quad (4)$$

$$AP\ (\%) = \left(\frac{W_2 - W_1}{W_2 - W_3}\right).100 \quad (5)$$

where W_w is the weight of the moist green body (in g), W_d is the weight of the dried pressed body (in g), W_1 is the dried fired body weight (in g), W_2 is the weight of the moist fired body (in g), W_3 is the immersed fired body weight (in g), L_o is the initial length of the specimen after formation by pressing (in mm), L_d is the length of the specimen after oven drying (in mm), L_f is the length of the test specimen after firing (in mm), F is the applied load (in N), and S is the area of application of the load (in m^2).

The compression test for the specimens was conducted in a universal 100 kN machine by EMIC Corporation at the Laboratory of Mechanical Tests of the IFES Vitória campus.

III. RESULTS AND DISCUSSION

3.1 Samples A, B, and C

3.1.1 Granulometric analysis

The particle-size distribution curves for the raw materials are presented in Figures 1, 2, and 3. Table 2 presents the specific ranges for the determination of the clay, silt, and sand granulometric fractions according to technical standard NBR 6502 (ABNT, 1995).

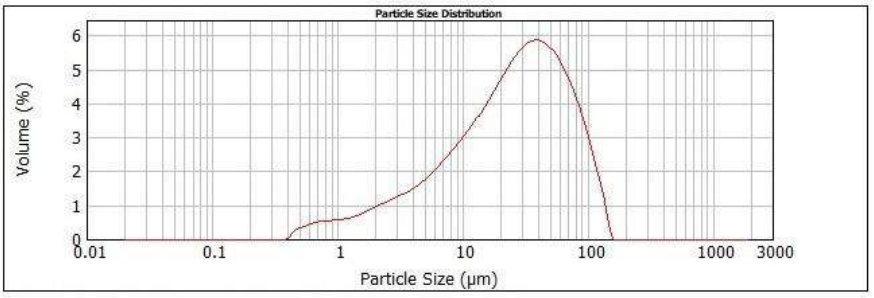

Figure 1: Sample A particle size distribution

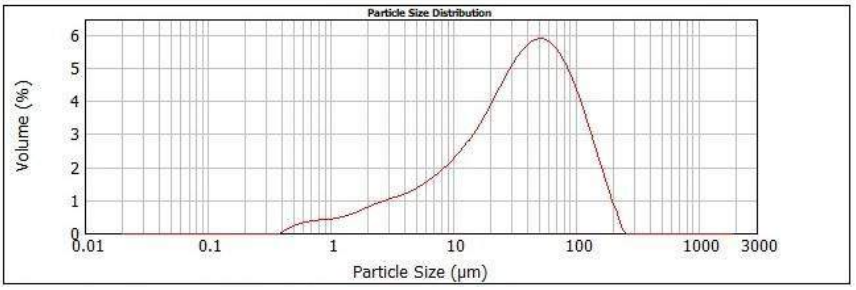

Figure 2: Sample B particle size distribution

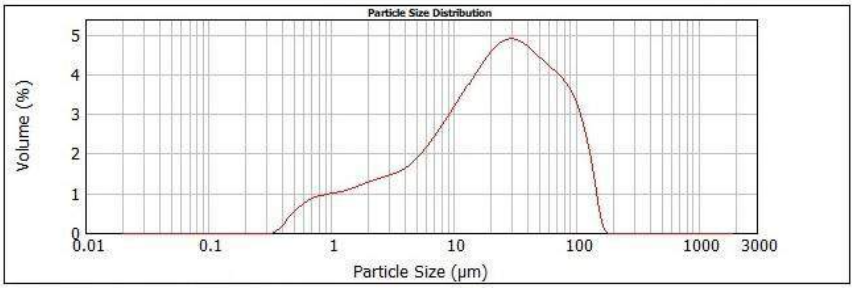

Figure 3: R sample particle size distribution

Table 2: Particle size classification – rocks and soils (adapted from ABNT NBR 6502:95)

Particle size classification	Grain diameter (μm)
Clay	< 2
Silt	2–60
Fine sand	60–200
Average sand	200–600

Analysis of the granulometric curves following technical standard NBR 6502 (ABNT, 1995) shows that samples A and B contain a small percentage of particles with granulometry values below 2 μm, and that sample A has a higher volumetric percentage than sample B of this clay material. This may be related to the higher clay content of kaolinite in sample A, and is indicative of a higher plasticity of sample A.

Both sample A and sample B contain a significant fraction corresponding to silt (2 to 60 μm). Sample B has a larger fraction of coarser material (fine sand) and a medium-range sand fraction that is not present in sample A. This may indicate a lower plasticity for sample B.

In contrast, the R sample has a high content of fine particles, which constitutes a nonplastic and inert material. Such a high content can contribute to a reduction in plasticity of the ceramic, and consequently a reduction in cracking susceptibility.

3.1.2 Plasticity

The plasticities of the samples were evaluated by means of the Atterberg limits and are presented in Table 3. Analysis of the data confirms that sample A is more plastic than sample B, which is in agreement with the results of the particle size analysis.

Table 3: Atterberg limits and plasticity index for samples A and B

		Samples	
		A	B
Atterberg limits	LL (%)	56	44
	PL (%)	30	31
	PI (%)	26	13

Based on the results presented in Table 3, sample A has high plasticity while sample B has low plasticity. If a clay has high water content, the paste can lose the ability to retain its shape due to its excessively fluidity. If a clay has low water content, the paste will be less fluid and more difficult to work (Andrade et al., 2011). To improve the processing of ceramic bricks, the supplier company mixes material A with material B with a composition of 3A-4B (42.85% wt A – 57.15% wt B).

3.1.3 X-ray diffraction

The diffractograms of samples A, B, and R are shown in Figures 4, 5, and 6, respectively.

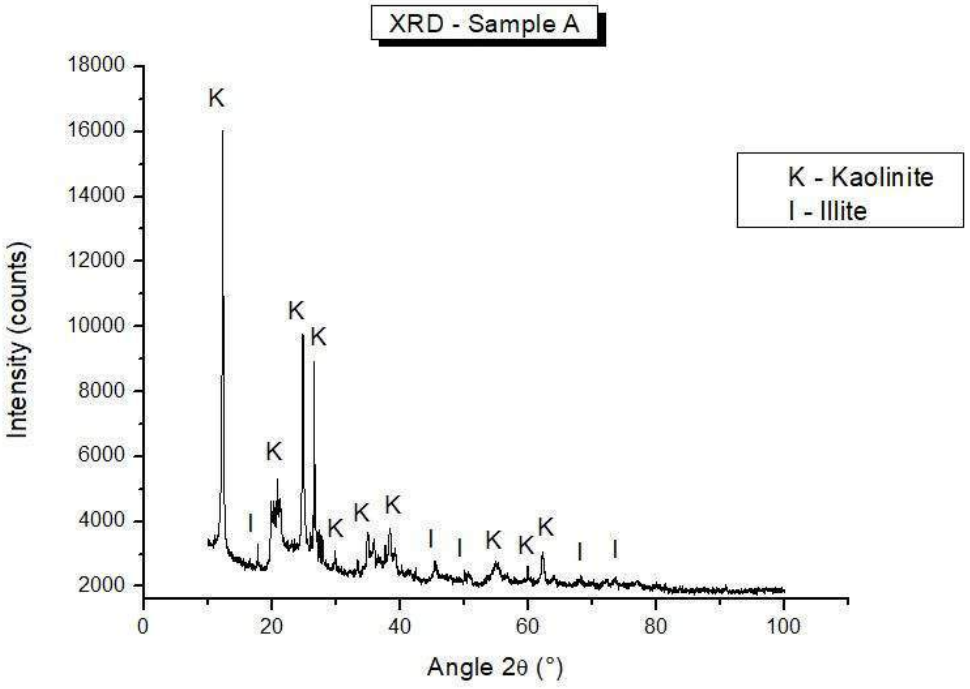

Figure 4: Sample A X-ray diffractogram

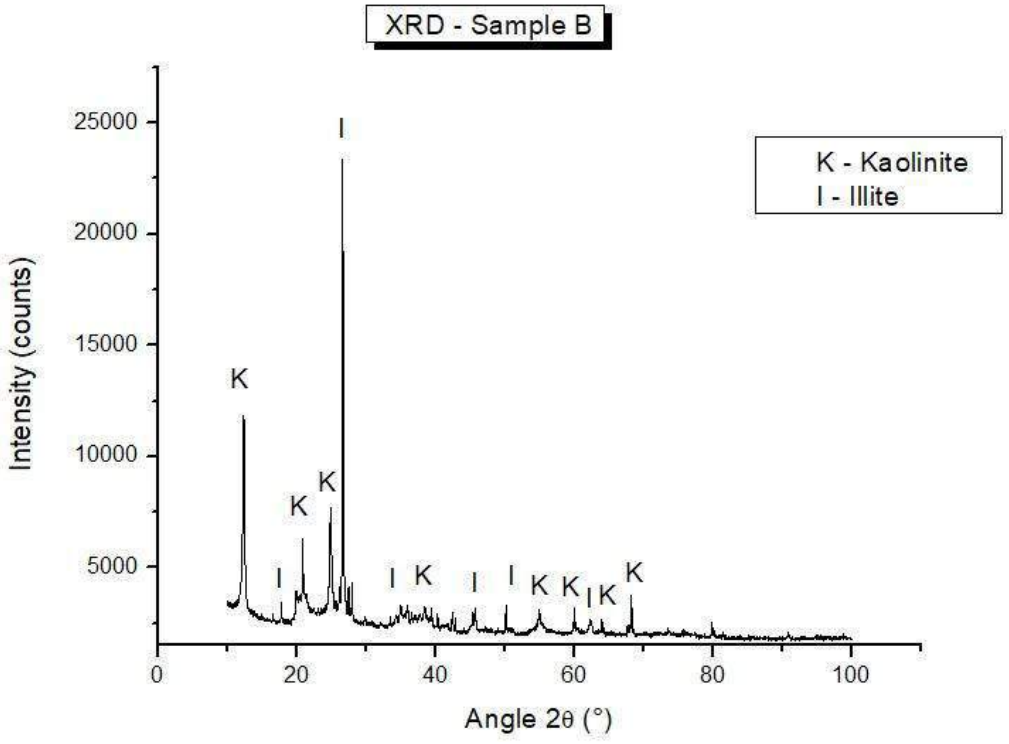

Figure 5: Sample B X-ray diffractogram

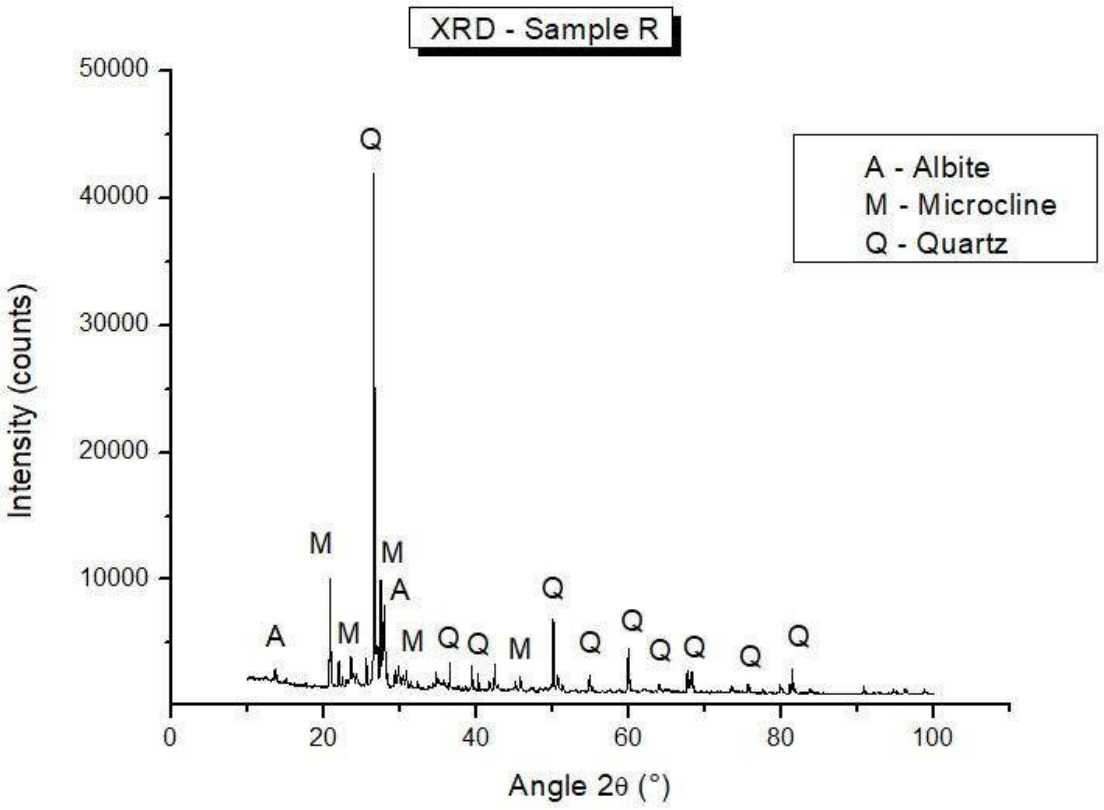

Figure 6: Sample R X-ray diffractogram

For samples A and B, it is possible to identify common peaks that confirm the presence of crystalline phases of kaolinite and illite. In addition to these phases, sample B presents characteristic peaks of muscovite mica, which is a mineral with lamellar morphology that may lead to defects in ceramic pieces and consequently a reduction in mechanical resistance. However, this mineral could act as a flux owing to the presence of alkaline oxides, as long as it contains particles of reduced size.

Figure 6 shows the presence of peaks for crystalline phases corresponding to quartz (SiO_2), potassium feldspar ($KAlSi_3O_8$ or microcline), and albite ($NaAlSi_3O_8$). The predominance of quartz indicates that the cutting residue of natural stones is mainly from granites because quartz is a predominant mineral in this type of stone.

3.1.4 Thermal analysis

Figures 7, 8, and 9 show the DSC/TG curves of samples A, B, and R. Figure 7 shows that an endothermic reaction occurs at approximately 100°C with a loss of mass corresponding to loss of moisture and adsorbed water. At 375°C, an exothermic reaction occurs with mass loss corresponding to loss of sulfides and combustion of organic matter. The glass transition of the material occurs at a temperature of 507°C, and the total mass loss for sample A amounts to 12.09%.

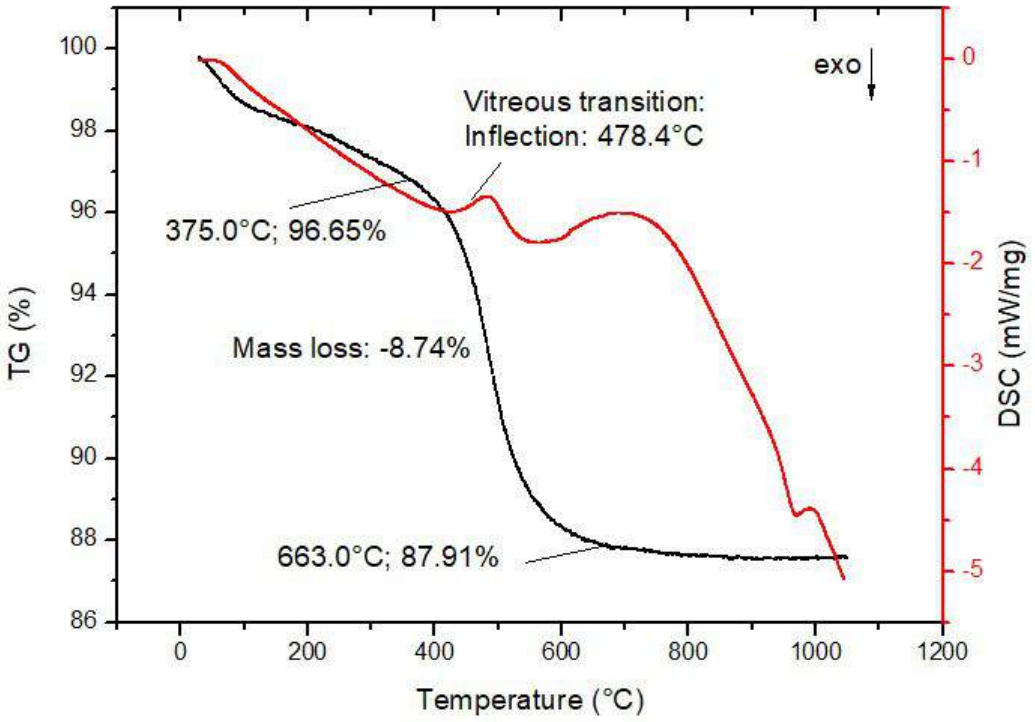

Figure 7: DSC/TG results for sample A.

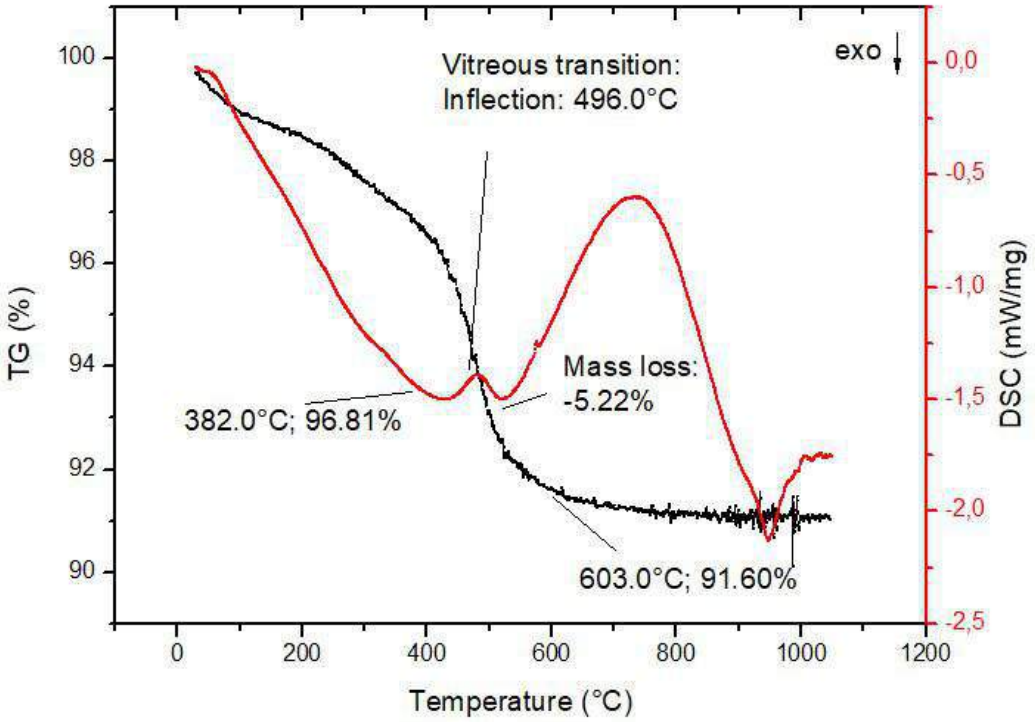

Figure 8: DSC/TG for sample B

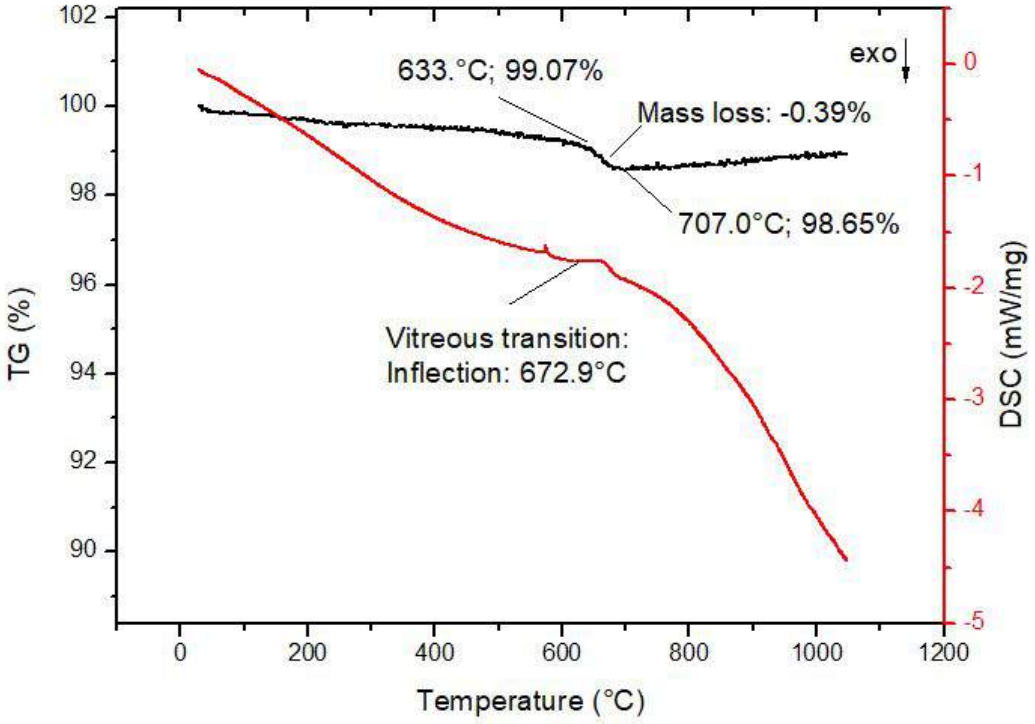

Figure 9: DSC/TG for sample R

The greatest mass loss (8.74%) is represented by an endothermic peak that occurs at a temperature of 663°C and is associated with the destruction of the crystalline lattice of the clay minerals. The water of the lattice, such as that found between the layers of kaolinite crystals, is part of the crystal structure; the loss results from the removal of hydroxyl from the clay minerals. (Rapid water outflow from kaolinite, a dehydroxylation reaction, is the condition under which metacaulinite is formed.)

According to Vieira et al. (2003), a ceramic is well suited for ceramic industrial processing if the mass loss during firing is between 5% and 7%. They also report that a high mass loss is typical of very plastic clays and is one of the main factors that give high porosity to the ceramic after the burning process.

Figure 8 indicates that the total mass loss for sample B is lower than that for sample A, which is expected because the plasticity of sample B is also lower. The largest mass loss, 5.22%, occurs between the temperatures of 382°C and 603°C, and the glass transition occurs at a temperature of 498.7°C; the total mass loss during the process is 8.40%, which does not fall within the interval classified by Vieira et al. (2003) as well-suited for industrial processing.

Figure 9 shows that, for sample R, there is a small loss of mass (0.39%) in an endothermic peak between the temperatures of 633°C and 707°C, which can be attributed to the elimination of water as micaceous mineral constituent. This endothermic peak is associated with the allotropic transformation of quartz. The glass transition occurs at 672.2°C, which is higher than the transition temperature of samples A and B.

3.1.5 Chemical analysis

Table 4 shows the chemical composition for samples A, B, and R.

Table 4: Results of chemical composition for samples A, B, and R

Chemical	Chemical composition (%)		
	Sample A	Sample B	Sample R
SiO_2	50.54	52.16	65.75
Al_2O_3	34.52	46.49	17.53
Fe_2O_3	8.86	0.58	4.62
K_2O	2.90	0.45	5.39
CaO	-	0.13	3.22
Na_2O	-	-	1.70
MgO	1.55	-	0.74
BaO	-	0.11	-
TiO_2	1.27	0.01	0.40
P_2O_5			0.32
MnO	0.11	-	0.06
SO_3	0.10	0.03	0.21
ZrO_2	0.10	0.01	-
Rb_2O	0.02	-	0.02
ZnO	0.01	0.01	0.01
SrO	0.01	0.01	0.02
CuO	-	0.01	-
Y_2O_3	0.01	0.01	0.01
Ga_2O_3	-	0.01	-

The results show that samples A and B are mainly composed of SiO_2 and Al_2O_3, totaling 85.07% for sample A and 98.65% for sample B, indicating that these samples contain kaolinite as the predominant clay mineral.

There is also a predominance of SiO_2, Al_2O_3, and Fe_2O_3 oxides, which typically represents a clay-based raw material composition for red ceramics. According to Pinheiro and Holanda (2010), the high percentage of Al_2O_3, which is present mainly in sample B, tends to increase the refractoriness (or heat resistance) of the clays.

Sample B has a low content of Fe_2O_3 (0.58%), making it possible to obtain products with light coloration because this oxide is the main contributor to the reddish color of the ceramic. In terms of silicon oxide (SiO_2), sample A has a lower content, indicating a higher plasticity. The alkaline compound K_2O is present in greater quantities in sample A. K_2O, which is generally present in the form of feldspar, is important for densification of red ceramics and increases the mechanical resistance in the sintering process. The alkaline-earth compounds (CaO and MgO) have a fluxing effect that facilitates the formation of the liquid phase, which is necessary for the consolidation of particles and which consequently increases the linear retraction (or shrinkage) in the burning process.

The sample R has a SiO_2 content of 65.75%, indicating that the residue is predominantly from granitic rocks, corroborating the XRD results.

3.1.6 Morphological analysis

Figures 10, 11, and 12 present scanning electron microscope images at magnifications of 1000 and 5000 times making it possible to analyze the size and shape of the grains of the raw materials used.

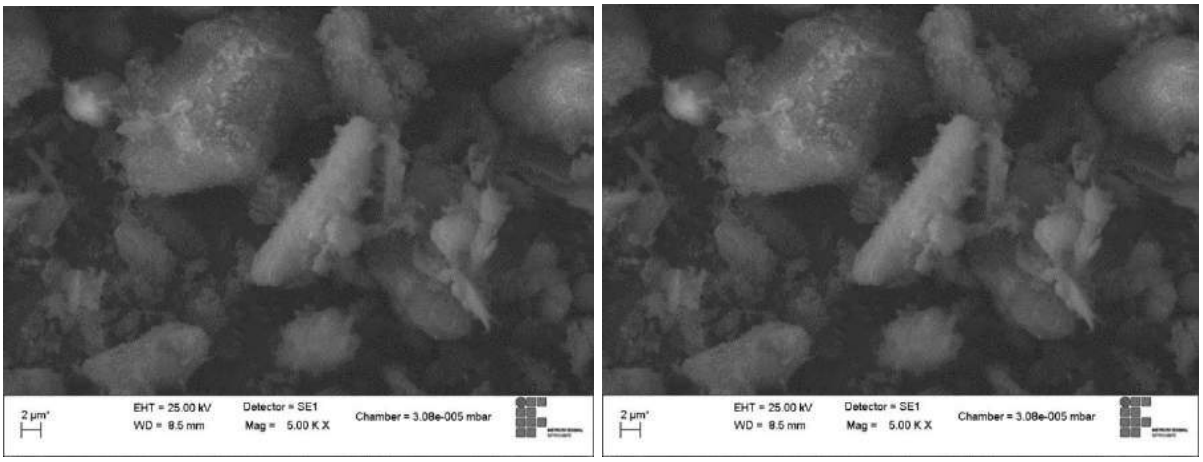

(a) 1000X (b) 5000X

Figure 10: SEM images for sample A

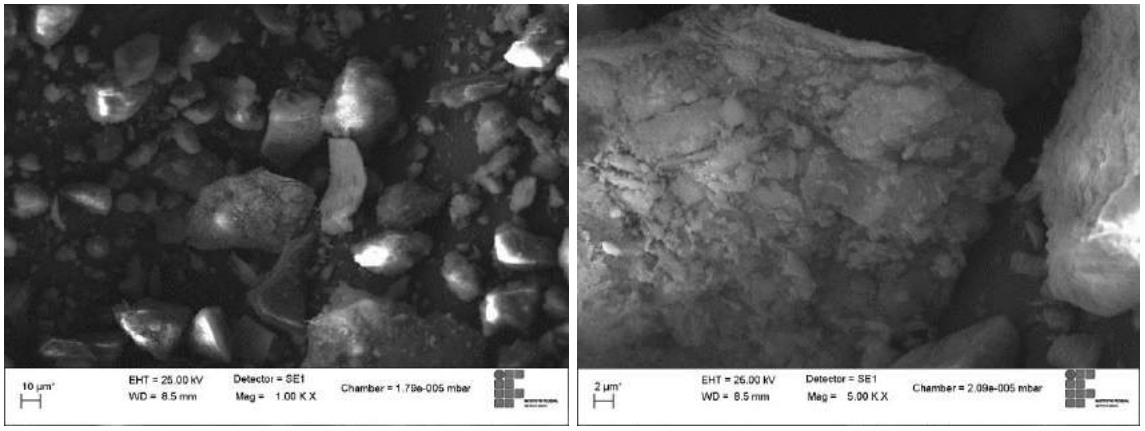

(a) 1000X (b) 5000X

Figure 11: SEM images for sample B

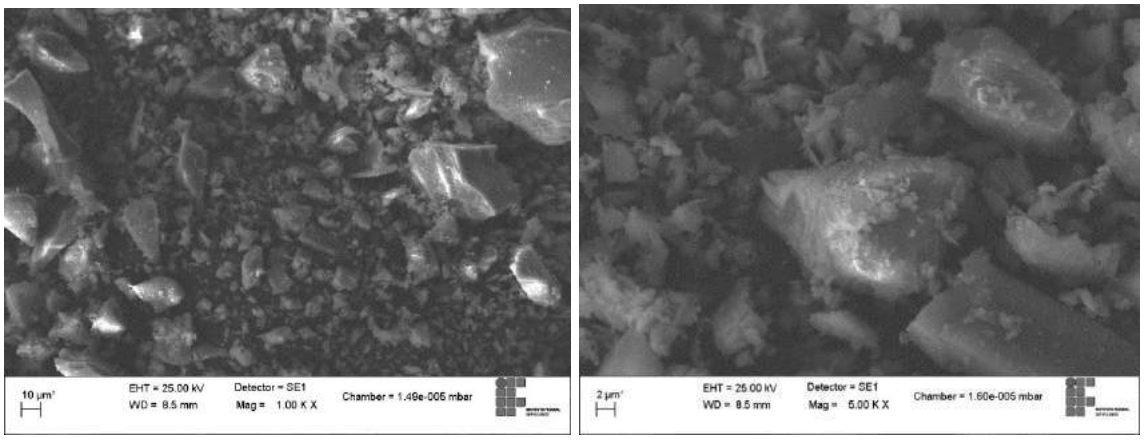

(a) 1000X (b) 5000X

Figure 12: SEM images for sample R

Figures 10 and 11 show the electron microscopy images for samples A and B, respectively. Analysis of these images reveals that this material contains particles of different sizes and morphology, and that these particles are well aggregated, which is indicative of high plasticity, a property already identified through the determination of the Atterberg limits.

For sample R, the micrometric size of the particles and their wide size distribution are shown in Figure 12. These images show well-delineated quartz particles with angular edges and irregular morphology as well as porous agglomerates. The fine particles contained in the residue can, at an appropriate percentage, contribute to reducing the plasticity and consequently the appearance of cracks in ceramics, and favor the dissolution of quartz during the firing stage.

3.2 Samples TR, T1, and T2

3.2.1 Particle size distribution

Figures 13, 14 and 15 show the grain-size curves for the TR, T1, and T2 samples, respectively.

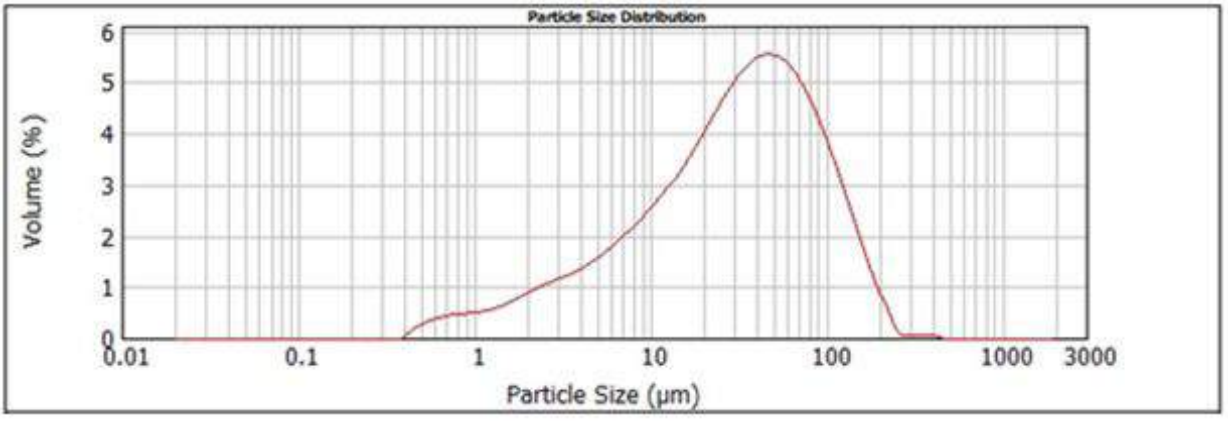

Figure 13: Particle size distribution for TR

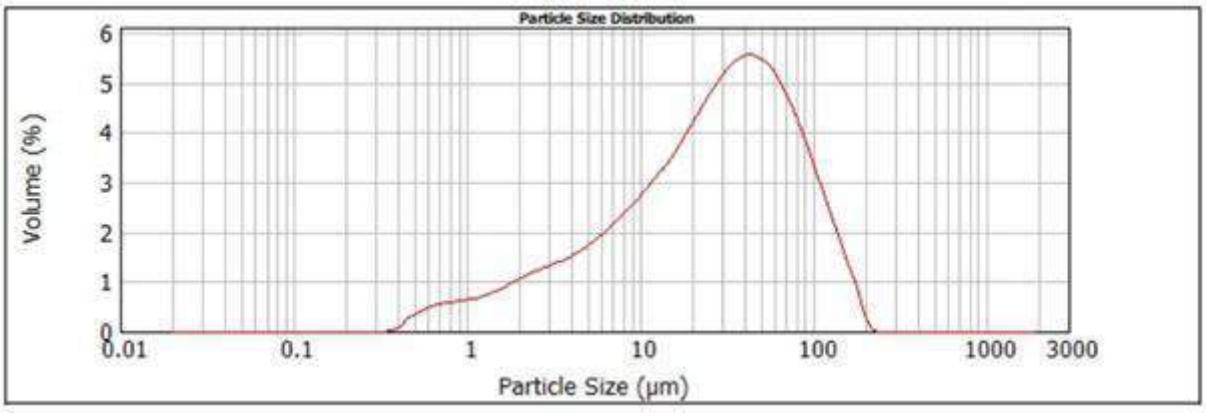

Figure 14: Particle size distribution for T1

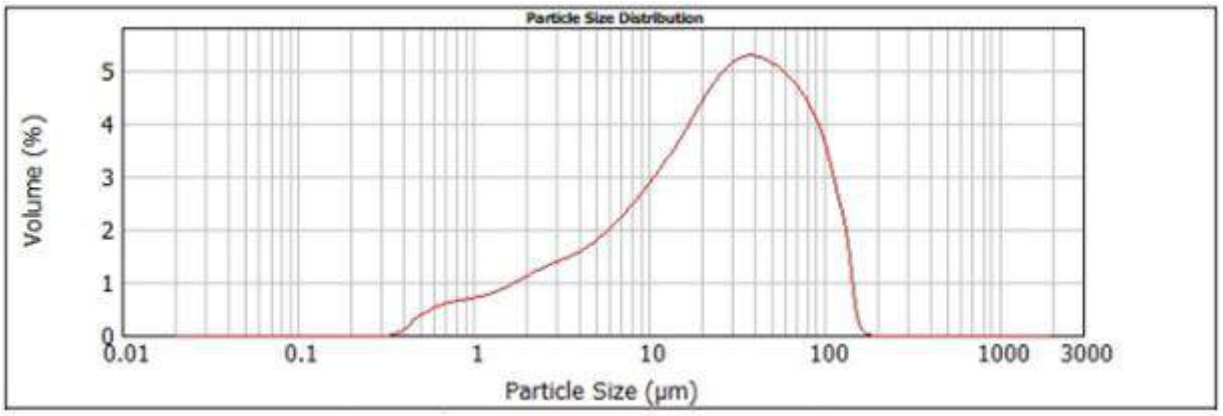

Figure 15: Particle size distribution for T2

The data presented in Table 2 and in Figures 13, 14 and 15 shows that the ceramic masses that are represented by the three samples are predominantly silty, and that the reference sample contains a larger fraction of the coarser material.

The plasticity of the samples was assessed using the Atterberg limits, and the results are presented in Table 5.

3.2.2 Atterberg limits

Table 5: Atterberg limits and plasticity index of samples TR, T1, and T2

Content		Samples		
		TR	T1	T2
Atterberg limits	LL (%)	52	43	38
	PL (%)	30	25	24
	PI (%)	22	18	14

Table 5 indicates that the addition of cutting stone residue decreases the plastic index for both T1 and T2 samples. With lower water content, pastes from T1 and T2 samples can lead to cracks during extrusion processing.

3.2.3 Thermal analysis

Figures 16, 17 and 18 provide the DSC/TG curves for the TR, T1, and T2 samples, respectively.

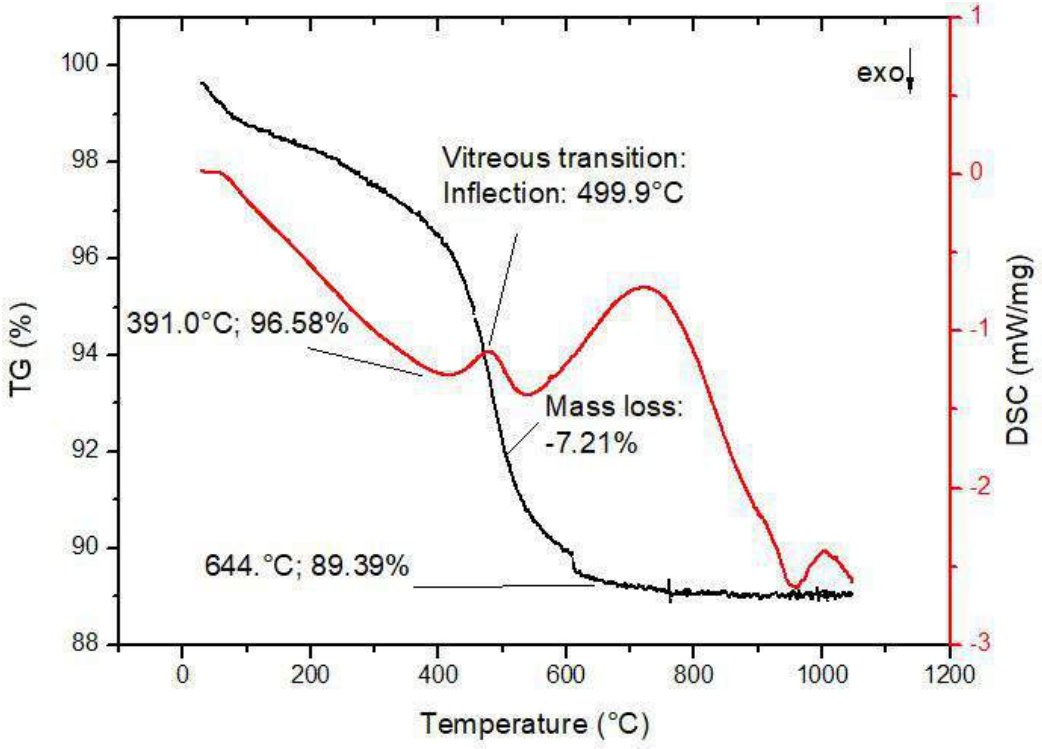

Figure 16: DSC/TG results for TR

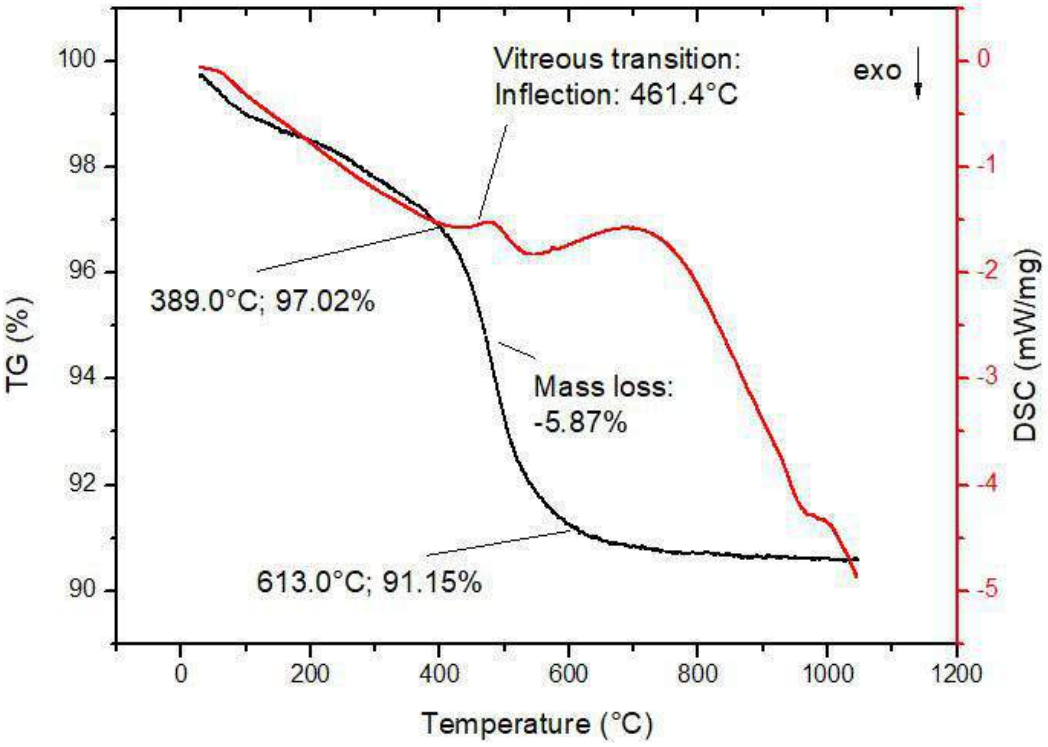

Figure 17: DSC/TG results for T1

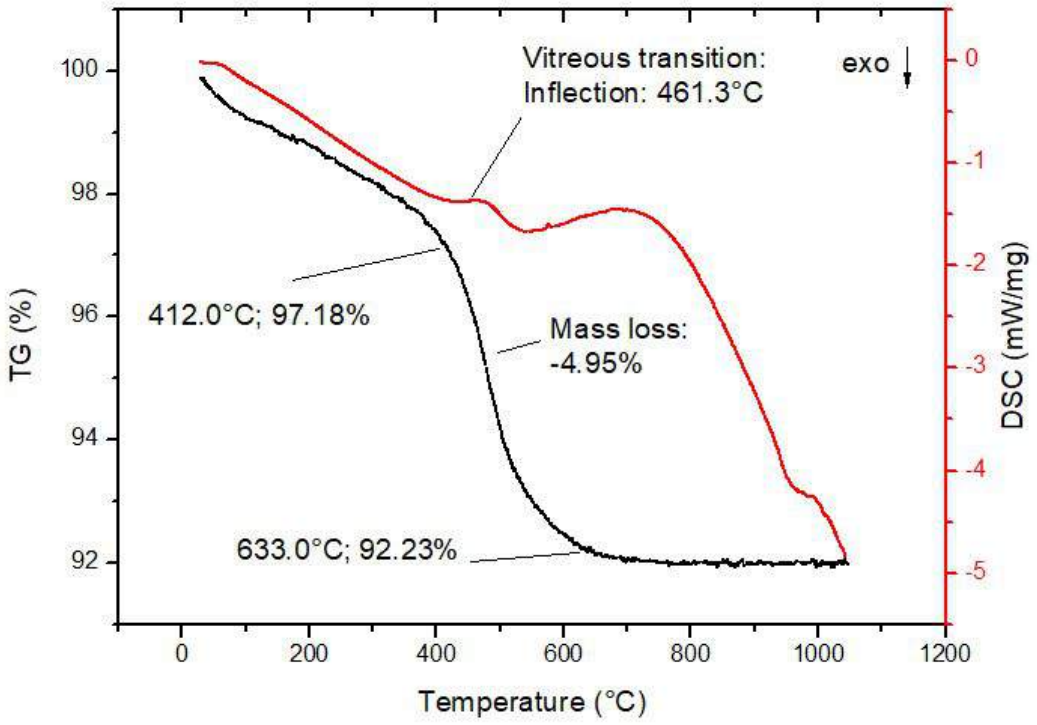

Figure 18: DSC/TG results for T2

These figures show that the smallest mass loss occurs for sample T2, and the greatest occurs for sample TR, which indicates the possibility of a greater retraction during burning of the reference sample and a smaller retraction for sample T2.

3.2.4 Morphological analysis

Figures 19, 20, and 21 show scanning electron microscopy images of the samples TR, T1, and T2 at 1000X and 5000X scales, where a variety of shapes and sizes can be observed for these material compositions as well as some agglomeration between grains. For sample T1, the images show a more closed distribution in which the more varied sizes of the grains pack together provide a denser material.

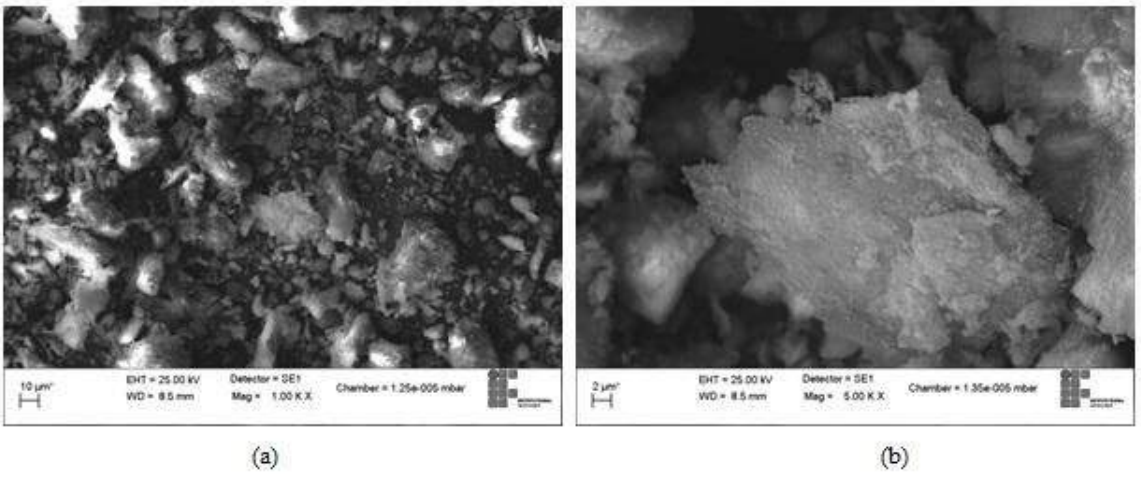

Figure 19: SEM images for sample TR

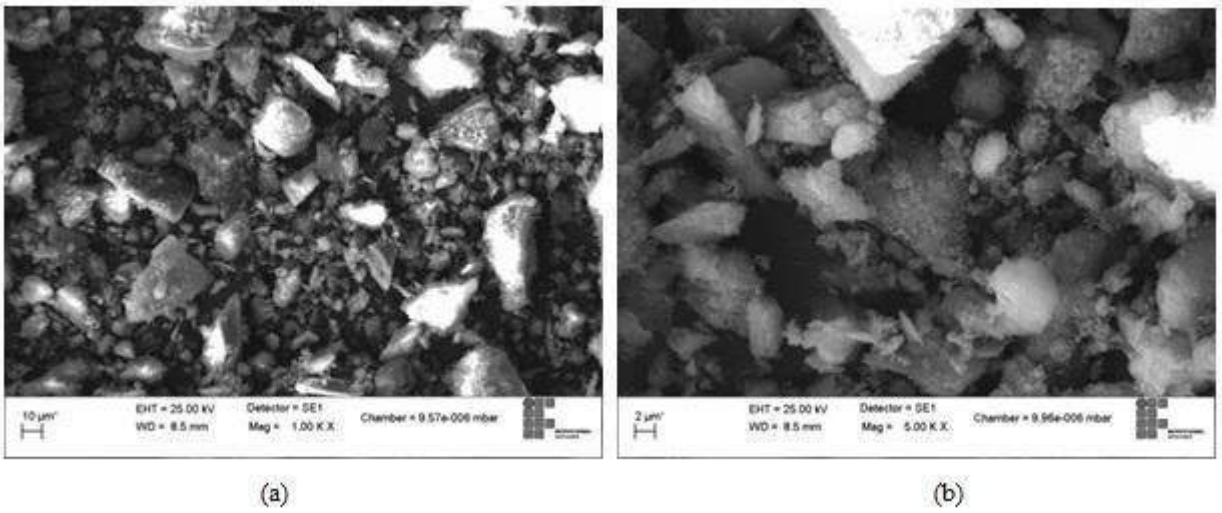

(a) (b)

Figure 20: SEM images for sample T1

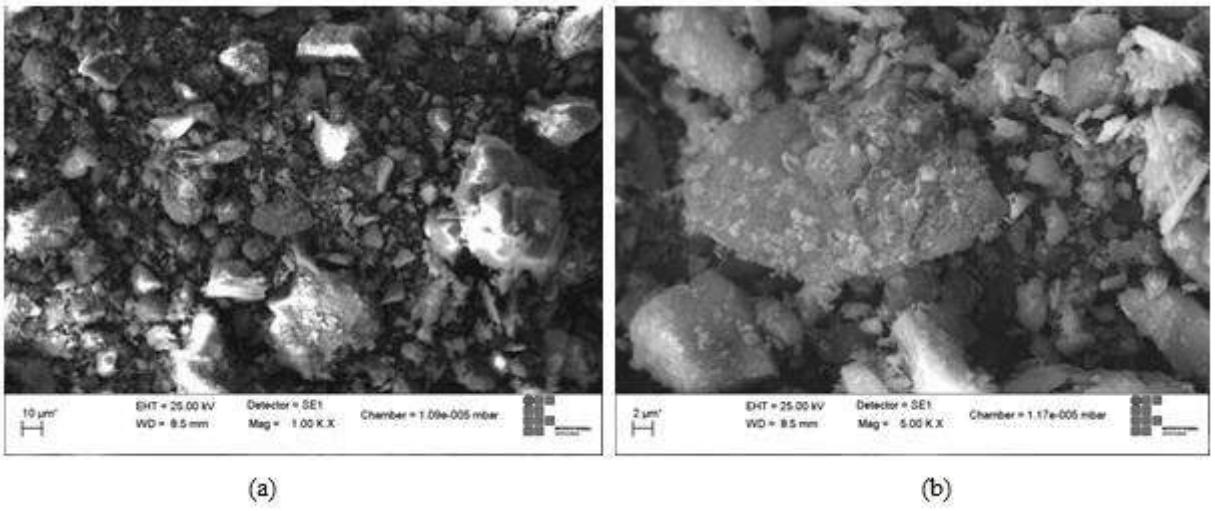

(a) (b)

Figure 21: SEM images for sample T2

3.2.5 Physical characterization

The moisture content required to determine mixing plasticity (for adequate formation of the ceramic mass) and the linear drying shrinkage suffered during the oven-drying process were determined as arithmetic means for 60 test specimens per sample, the results of which are presented in Table 6.

Table 6: Results of moisture content and linear drying shrinkage for samples TR, T1, and T2

Sample	MC (%)	LDS (%)
TR	10.33 ± 3.21	0.38 ± 0.21
T1	10.85 ± 0.58	0.33 ± 0.19
T2	10.14 ± 0.76	0.43 ± 0.22

The moisture contents of TR, T1, and T2 were similar in value; they were less than 30%, which is considered low moisture, and could lead to cracks from drying and burning.

To determine the water absorption (WA), apparent porosity (AP), apparent density (AD), linear firing shrinkage (LFS), and compressive strength (CS) after firing, the arithmetic means for 15 specimens per sintering temperature were calculated for each sample. The results of the physical and mechanical characterization are shown in Table 7.

Table 7: Results of physical properties for samples TR, T1, and T2

Sample	MC (%)	LDS (%)
TR	10.33 ± 3.21	0.38 ± 0.21
T1	10.85 ± 0.58	0.33 ± 0.19
T2	10.14 ± 0.76	0.43 ± 0.22

Comparing results for TR and T1, water absorption increases with the inclusion of 14% residue in the T1 sample (see Table 1) for the first two temperatures that were studied, and is similar at the highest temperature. However, the WA continues to decrease with the increase of the residue content (to 28.5% in the T2 sample), reaching a value similar to that of TR at a temperature of 850°C. This tendency for a decrease of the absorption with an increase in residue content may be due to an improvement in packing or a reduction in the amount of water of formation, and consequently a reduction in loss of mass during burning. It is also interesting to note that there is a more pronounced reduction in water absorption at the lower temperature (850°C). According to technical standard NBR 15270-1 (ABNT, 2005), the water absorption value for bricks should be between 8% and 22%. All the water absorption results, regardless of the sintering temperature or sample, meet this specification.

The apparent porosity of the material follows a similar behavior to that of water absorption; however, it shows insignificant changes with increase in residue content at the temperature of 950°C.

The reduction in water absorption and the decreasing porosity occur as a consequence of the fluxing action of the residue and the formation of a liquid phase in the sintering process. This liquid fills the pores and thickens the ceramic body. The trends in WA and AP indicate that the amount of phase generated contributes to reducing the porosity.

The apparent density decreases for the two lower temperatures with the inclusion of 14% residue in the T1 sample, and has a slight increase at the temperature of 950°C. The AD continues to increase with the increase in residue content for the three temperatures, verifying the results of the previous analyses.

The linear firing shrinkage increases with the inclusion of 14% residue at a temperature of 850°C and decreases with a further increase in residue content. At the other temperatures (900°C and 950°C), LFS decreases for the two residue contents (14% and 28.5%). When compared to values at the other temperatures, for the reference sample the LFS is lowest at the temperature of 850°C, and close to the T1 and T2 values at the three temperatures studied.

The compressive strength shows similar values for the reference sample at the three temperatures, and higher values at the higher temperatures for the T1 and T2 samples. In addition, CS decreases with the inclusion of residue at the three temperatures and continues to decrease with increasing residue content. This reduction in CS can be associated with changes in the quartz phases that cause an increase in the volume of the

ceramic body, generating microcracks that act as tension concentrators and reduce the mechanical strength. According to technical standard NBR 15270-1 (ABNT, 2005), the values of CS should be equal to or greater than 1.5 MPa (for bricks used horizontally) or 3.0 MPa (for bricks used vertically). Thus, the results of CS were superior to that specified in the Brazilian standard, regardless of the sample and the sintering temperature.

VI. CONCLUSIONS

This work evaluated how the replacement of the less plastic clay by natural stone waste influences the physical and mechanical properties of sintered ceramic bodies. Results show the following:

- Samples A and B exhibit high plasticity because they consist of kaolinite and illite, which are clay minerals that impart plasticity to the clays and require a greater amount of water for formation.
- According to Vieira et al. (2003), for a ceramic mass to be well suited to industrial processing, the mass loss during firing should be between 5 and 7%. The ceramic mass that comes closest to these values is the one with the highest residue content, indicating that an increase in the residue content is possible such that the loss of mass falls within the desired range and consequently less water is required for formation.
- The inclusion of 28.5% residue in sample B results in denser ceramic masses owing to the inherent characteristics of this material that, in addition to acting as a plasticity reducer, can act as a glass-phase former, either filling pores or serving as a glassy matrix of crystalline grains.
- The T2 sample, which contained the larger amount of residue, gave rise to less porous ceramic bodies, and with low percentages of water absorption is consequently ideal for producing coatings, bricks, sandstone, and other products that require low absorption.
- The ceramic masses that were obtained by mixing samples A, B, and R can reduce the possibility of defects arising from excessive plasticity, because the residue acts as a plasticity reducer, reducing the amount of water needed for formation.
- Even though many properties were improved with the insertion of the residue, it is always necessary to evaluate the characteristics and properties of the material and to comply with the specific standard for each final desired product.
- The ceramic masses produced by mixing samples A, B, and R meet the specifications of water absorption and compressive strength described in the Brazilian technical standard NBR 15270-1 (ABNT, 2005).

ACKNOWLEDGEMENTS

The authors would like to thank Cerâmica Adélio Lubiana Ltda. and Centro de Tratamento de Resíduos (CTR) for their donation of raw materials; the Academic Unit of Materials Engineering of the Federal University of Campina Grande for conducting the thermogravimetric and X-ray fluorescence analyses; and the Federal Institute of Education, Science, and Technology of Espírito Santo for the financial support.

REFERENCES

1. Acchar, W., Vieira, F.A., Segadães, A.M., 2006. Using ornamental stone cutting rejects as raw materials for red clay ceramic products: Properties and microstructure development. Mater. Sci. Eng. A 435–436, 606–610.
2. Andrade, F.A., Al-Qureshi, H.A., Hotza, D., 2011. Measuring of plasticity clays: A review. Appl. Clay Sci. 51, 1–7.
3. Alyamac, K.E., Ghafari, E., Ince, R., 2017. Development of eco-efficient self-compacting concrete with waste marble powder using the response surface method. J. Cleaner Prod. 144, 192–202.
4. André, A., de Brito, J., Rosa, A., Pedro, D., 2014. Durability performance of concrete incorporating coarse aggregates from marble industry waste. J. Cleaner Prod. 65, 389–396.

5. Aydin, G., Kaya, S., Karakurt, I., 2017. Utilization of solid-cutting waste of granite as an alternative abrasive in abrasive waterjet cutting of marble. J. Cleaner Prod. 159, 241–247.
6. Boltakova, N.V., Faseeva, G.R., Kabirov, R.R., Nafikov, R.M., Zakharov, Y.A., 2017. Utilization of inorganic industrial wastes in producing construction ceramics. Review of Russian experience for the years 2000–2015. Waste Manage. 60, 230–246.
7. Brazilian Association of Technical Standards (ABNT), NBR 6459: Soil – Liquid limit determination, 2017.
8. Brazilian Association of Technical Standards (ABNT), NBR 6502: Rocks and soils – Terminology, 1995.
9. Brazilian Association of Technical Standards (ABNT), NBR 7180: Soil – Plasticity limit determination, 2016.
10. Brazilian Association of Technical Standards (ABNT), NBR 15270-1: Ceramic components – Clay blocks and bricks for masonry Part 1: Requirements, 2005.
11. Coletti, C., Maritan, L., Cultrone, G., Dalconi, M.C., Hein, A., Molina, E., Mazzoli, C., 2018. Recycling trachyte waste from the quarry to the brick industry: Effects on physical and mechanical properties, and durability of new bricks. Constr. Build. Mater. 166, 792–807.
12. Dondi, M., Cappelletti, P., D'Amore, P., de Gennaro, R., Graziano, S.F., Langella, A., Raimondo, M., Zanelli, C., 2016. Lightweight aggregates from waste materials: Reappraisal of expansion behavior and prediction schemes for bloating. Constr. Build. Mater. 127, 394–409.
13. Hossiney, N., Das, P., Mohan, M.K., George, J., 2018. In-plant production of bricks containing waste foundry sand – a study with Belgaum foundry industry. Case Stud. Constr. Mater. 9, e00170.
14. Lu, J., Li, Y., Zou, C., Liu, Z., Wang, C., 2018. Effect of sintering additives on the densification, crystallization and flexural strength of sintered glass-ceramics from waste granite powder. Mater. Chem. Phys. 216, 1–7.
15. Marras, G., Bortolussi, A., Peretti, R., Careddu, N., 2017. Characterization methodology for re-using marble slurry in industrial applications. Energy Procedia 125, 656–665.
16. Medina, G., Saez del Bosque, I.F., Frías, M., Sanchez de Rojas, M.I., Medina, C., 2017. Granite quarry waste as a future eco-efficient supplementary cementitious material (SCM): Scientific and technical considerations. J. Cleaner Prod. 148, 467–476.
17. Menezes, R.R., Ferreira, H.S., Neves, G.A., Lira, H.L., Ferreira, H.C., 2005. Use of granite sawing wastes in the production of ceramic bricks and tiles. J. Eur. Ceram. Soc. 25, 1149–1158.
18. Menezes, R.R., Malzac Neto, H.G., Santana, L.N.L., Lira, H.L., Ferreira, H.S., Neves, G.A., 2008. Optimization of wastes content in ceramic tiles using statistical design of mixture experiments. J. Eur. Ceram. Soc. 28, 3027–3039.
19. Nunes, J.M.G., Kautzmann, R.M., Oliveira, C., 2014. Evaluation of the natural fertilizing potential of basalt dust wastes from the mining district of Nova Prata (Brazil). J. Cleaner Prod. 84, 649–656.
20. Pinheiro, B.C.A., Holanda, J.N.F., 2010. Effect of the firing temperature on some mechanical properties of red ceramic. Cerâmica, 56, 237–243.
21. Ribeiro, C.E.G., Rodriguez, R.J.S., Carvalho, E.A., 2017. Microstructure and mechanical properties of artificial marble. Constr. Build. Mater. 149, 149–155.
22. Sardinha, M., de Brito, J., Rodrigues, R., 2016. Durability properties of structural concrete containing very fine aggregates of marble sludge. Constr. Build. Mater. 119, 45–52.
23. Sardou Filho, R., Matos, G.M.M., Mendes, V.A., Iza, E.R.H.F., Atlas of dimension stones of the Espírito Santo state. Brasília : CPRM, 2015.1 atlas (353 p.).

24. Segadães, A.M., Carvalho, M.A., Acchar, W., 2005. Using marble and granite rejects to enhance the processing of clay products. Appl. Clay Sci. 30, 42–52.
25. Soltan, A.M.M., Kahl, W.A., Raoof, F.A., El-Kaliouby, B.A.H., Serry, M.A.K., Abdel-Kader, N.A., 2016. Lightweight aggregates from mixtures of granite wastes with clay. J. Cleaner Prod. 117, 139–149.
26. Torres, P., Fernandes, H.R., Olhero, S., Ferreira, J.M.F., 2009. Incorporation of wastes from granite rock cutting and polishing industries to produce roof tiles. J. Eur. Ceram. Soc. 29, 23–30.
27. Vieira, C.M.F., Soares, T.M., Monteiro, S.N., 2003. Ceramic bodies for roofing tiles: characteristics and firing behavior. Cerâmica 49, 245–250.
28. Vieira, C.M.F., Soares, T.M., Sánchez, R., Monteiro, S.N., 2004. Incorporation of granite waste in red ceramics. Mater. Sci. Eng. A 373, 115–121.
29. Yeşilaya, S., Çakıb, M., Ergun, H., 2017. Usage of marble wastes in traditional artistic stoneware clay body. Ceramics Int. 43, 8912–8921
30. Zhang, L., 2013. Production of bricks from waste materials – A review. Constr. Build. Mater. 47, 643–655.